

A LoD of Gaussians: Unified Training and Rendering for Ultra-Large Scale Reconstruction with External Memory

FELIX WINDISCH, Graz University of Technology, Austria

LUKAS RADL, Graz University of Technology, Austria

THOMAS KÖHLER, Graz University of Technology, Austria

MICHAEL STEINER, Graz University of Technology, Austria

DIETER SCHMALSTIEG, Graz University of Technology, Austria and University of Stuttgart, Germany

MARKUS STEINBERGER, Graz University of Technology, Austria and Huawei, Austria



Fig. 1. We introduce a fully hierarchical 3D Gaussian representation trained directly across unstructured, multi-scale image sets—including street-level and aerial views—without scene partitioning. Our method maintains a consistent global scene model, eliminating boundary artifacts typical of chunked approaches. A hybrid Level-of-Detail system combines Gaussian hierarchies with Sequential Point Trees, enabling dynamic, view-dependent streaming and LoD selection. The entire model resides in external memory, with only a small, adaptive subset loaded on demand, allowing real-time rendering and training of 60M+ Gaussians on consumer GPUs ($\leq 24\text{GB VRAM}$). This is the first approach to achieve bounded-memory training and rendering of city-scale Gaussian splats at interactive rates.

Gaussian Splatting has emerged as a high-performance technique for novel view synthesis, enabling real-time rendering and high-quality reconstruction

Authors' Contact Information: Felix Windisch, felix.windisch@tugraz.at, Graz University of Technology, Graz, Austria; Lukas Radl, lukas.radl@tugraz.at, Graz University of Technology, Graz, Austria; Thomas Köhler, t.koehler@tugraz.at, Graz University of Technology, Graz, Austria; Michael Steiner, michael.steiner@tugraz.at, Graz University of Technology, Graz, Austria; Dieter Schmalstieg, schmalstieg@tugraz.at, Graz University of Technology, Graz, Austria and University of Stuttgart, Stuttgart, Germany; Markus Steinberger, steinberger@tugraz.at, Graz University of Technology, Graz, Austria and Huawei, Graz, Austria.

Permission to make digital or hard copies of all or part of this work for personal or classroom use is granted without fee provided that copies are not made or distributed for profit or commercial advantage and that copies bear this notice and the full citation on the first page. Copyrights for components of this work owned by others than the author(s) must be honored. Abstracting with credit is permitted. To copy otherwise, or republish, to post on servers or to redistribute to lists, requires prior specific permission and/or a fee. Request permissions from permissions@acm.org.

© 2025 Copyright held by the owner/author(s). Publication rights licensed to ACM.
ACM XXXX-XXXX/2025/7-ART

<https://doi.org/10.1145/nnnnnnnnnnnnnn>

of small scenes. However, scaling to larger environments has so far relied on partitioning the scene into chunks—a strategy that introduces artifacts at chunk boundaries, complicates training across varying scales, and is poorly suited to unstructured scenarios such as city-scale flyovers combined with street-level views. Moreover, rendering remains fundamentally limited by GPU memory, as all visible chunks must reside in VRAM simultaneously. We introduce *A LoD of Gaussians*, a framework for training and rendering ultra-large-scale Gaussian scenes on a single consumer-grade GPU—without partitioning. Our method stores the full scene out-of-core (e.g., in CPU memory) and trains a Level-of-Detail (LoD) representation directly, dynamically streaming only the relevant Gaussians. A hybrid data structure combining Gaussian hierarchies with Sequential Point Trees enables efficient, view-dependent LoD selection, while a lightweight caching and view scheduling system exploits temporal coherence to support real-time streaming and rendering. Together, these innovations enable seamless multi-scale reconstruction and interactive visualization of complex scenes—from broad aerial views to fine-grained ground-level details.

CCS Concepts: • Computing methodologies → Rasterization; Visibility; Machine learning.

Additional Key Words and Phrases: Level of Detail, Gaussian Splatting, Large-Scale Reconstruction

ACM Reference Format:

Felix Windisch, Lukas Radl, Thomas Köhler, Michael Steiner, Dieter Schmalstieg, and Markus Steinberger. 2025. A LoD of Gaussians: Unified Training and Rendering for Ultra-Large Scale Reconstruction with External Memory. 1, 1 (July 2025), 12 pages. <https://doi.org/10.1145/nnnnnnnn.nnnnnnnn>

1 Introduction

Given a set of posed images of a 3D scene, the task of novel view synthesis (NVS) is to generate plausible images of the scene from unseen viewpoints. Early approaches achieved this via image-based blending [Zhang et al. 2019], but the introduction of Neural Radiance Fields (NeRF) [Mildenhall et al. 2020] marked a breakthrough, enabling high-quality results by optimizing an implicit volumetric scene representation through a multi-layer perceptron. More recently, 3D Gaussian Splatting (3DGS) [Kerbl et al. 2023] extended this paradigm to an explicit representation: a set of Gaussian primitives that are efficiently rasterized using splatting techniques [Zwicker et al. 2001], replacing costly ray marching and allowing real-time rendering with fast convergence.

Despite these advances, both NeRF and 3DGS remain constrained by memory bottlenecks when applied to large-scale environments. Prior methods address this by dividing scenes into smaller chunks [Chen et al. 2024b; Kerbl et al. 2024; Li et al. 2024; Lin et al. 2024; Liu et al. 2024a; Tancik et al. 2022; Xu et al. 2023], training each independently before merging results. While chunking strategies mitigate memory usage during training, they introduce several key limitations:

- (1) **View-chunk misalignment:** Camera views often span multiple chunks, especially in open environments or multi-scale datasets (e.g., combining aerial and street-level images). This makes chunk boundaries arbitrary and hard to define, complicating scene partitioning and training.
- (2) **Redundant overlap:** To avoid artifacts at chunk boundaries, regions are typically trained with significant overlap, which increases memory usage and prolongs training time.
- (3) **Asymmetric hardware demands:** Although chunking reduces memory requirements during training, rendering may require all visible chunks in memory simultaneously—often exceeding the capacity of the original training setup.

The simplest and most robust alternative to chunking is to avoid splitting altogether. With *A LoD of Gaussians*, we introduce a seamless pipeline that enables training and rendering of ultra-large-scale scenes directly—on a single consumer-grade GPU—without any form of scene partitioning. To handle scenes that exceed available VRAM, we store all Gaussian data in CPU RAM and dynamically stream only those visible from the current training view into GPU memory. However, a single far-away view could still require access to the full scene. To address this, we construct a hierarchical Level-of-Detail (LoD) model inspired by Kerbl et al. [2024], loading detail proportional to view distance. Maintaining this hierarchy during training is non-trivial, as Gaussian properties evolve dynamically.

We propose a novel hierarchy densification strategy, adapted from the MCMC-style spawning [Kheradmand et al. 2024], to support stable, progressive refinement. Efficient view-dependent selection from the hierarchy is challenging for large models. Instead of full tree traversal, we adopt Sequential Point Trees (SPTs) [Dachsbaecher et al. 2003], originally developed for point cloud LoD rendering. Our Hierarchical SPT version allows us to compute the correct LoD cut efficiently for rendering individual views and camera paths. Finally, to reduce CPU-GPU data transfer overhead, we introduce a lightweight caching system that tracks recently used Gaussians and reuses them across training iterations. In summary, we make the following contributions:

- (1) We propose a novel hierarchy densification strategy that enables dynamic expansion and restructuring of Gaussian representations during training.
- (2) We leverage the Sequential Point Tree (SPT) data structure and adapt it for large-scale Gaussian Splatting to perform fast, parallelizable LoD cuts for efficient training and real-time rendering.
- (3) We demonstrate, for the first time, how external memory can be used to train and render ultra-large Gaussian scenes seamlessly on consumer-grade GPUs.
- (4) We design a caching and view scheduling system that exploits temporal coherence to minimize data transfer overhead and improve training throughput.

2 Related Work

Large Scale Reconstruction. Reconstructing large-scale scenes from images has long been a central challenge in visual computing. Traditional approaches relied on Structure-from-Motion pipelines, such as *Building Rome in a Day* [Agarwal et al. 2009] and *COLMAP* [Schönberger and Frahm 2016], to recover geometry from unordered photo collections. Differentiable rendering techniques, notably NeRF [Mildenhall et al. 2020] and 3DGS [Kerbl et al. 2023], marked a paradigm shift by optimizing volumetric scene representations. Extensions of NeRF to large scenes typically employ scene partitioning [Tancik et al. 2022; Xu et al. 2023] or multi-GPU training strategies [Li et al. 2024]. Similarly, most large-scale 3DGS pipelines adopt chunk-based training: *Hierarchical 3DGS* [Kerbl et al. 2024] trains chunks independently and then merges them into a global LoD hierarchy; *CityGaussian* [Liu et al. 2024a] combines chunked training with per-chunk LoD selection using *LightGaussian* [Fan et al. 2024]; and *VastGaussian* [Lin et al. 2024] introduces decoupled appearance modeling and progressive partitioning. *Horizon-GS* [Jiang et al. 2024] integrates divide-and-conquer strategies with LoD mechanisms from [Ren et al. 2024], specifically targeting hybrid aerial/street-view datasets. *Grendel* [Zhao et al. 2024] avoids spatial chunking by distributing training images across GPUs, such that each device renders a disjoint screen region. Another research direction focuses on extracting geometric proxies from large-scale 3DGS scenes [Chen et al. 2024b; Li et al. 2025; Liu et al. 2025]. These methods leverage TSDF fusion and geometric losses to generate multiple meshes, which are fused and rendered efficiently using traditional rasterization.

Compression. Lowering memory consumption is essential to scaling 3DGS to larger scenes. Compression techniques typically fall into three overlapping categories: *compaction*, which reduces the number of Gaussians; *attribute compression*, which reduces the storage per primitive; and *structured representations*, which organize data to improve compressibility. Pure compaction strategies include [Cheng et al. 2024; Fang and Wang 2024; Kim et al. 2024; Liu et al. 2024c; Mallick et al. 2024; Ren et al. 2024]; hybrid methods that also compress attributes include [Fan et al. 2024; Girish et al. 2024; Papantonakis et al. 2024a; Wang et al. 2024b]; and pure attribute compression is addressed by [Niedermayr et al. 2024]. Methods combining all three dimensions include [Chen et al. 2024a; Lee et al. 2024], while [Liu et al. 2024b; Navaneet et al. 2023; Wang et al. 2024a; Ye et al. 2025] emphasize attribute compression with structural priors. Finally, Lu et al. [2023] focus on hierarchical anchoring. These techniques are largely orthogonal to our work—many are applied post hoc or modify densification policies—and could be combined with our pipeline for further gains in memory and performance.

Level-of-Detail Rendering. Level-of-detail techniques reduce the complexity of distant scene content to accelerate rendering. In the context of 3DGS, LoD approaches have been explored for enabling efficient rendering on memory-constrained or mobile devices. Compression-based strategies include attribute quantization via codebooks, pruning of low-impact Gaussians, and adapting the degree of spherical harmonics per primitive [Fan et al. 2024; Fang and Wang 2024; Huang et al. 2025; Niedermayr et al. 2024; Niemeyer et al. 2025; Papantonakis et al. 2024b; Seo et al. 2024]. *Scaffold-GS* [Lu et al. 2023] introduced learned feature vectors anchored to reference Gaussians, with an MLP generating associated Gaussians at render time. This concept was extended to hierarchical LoD rendering in *Octree-GS* [Ren et al. 2024], enabling real-time control over detail levels through spatial subdivision.

3 Preliminaries

We briefly review 3D Gaussian Splatting and describe its memory usage characteristics. We then introduce the key data structures we used: Gaussian hierarchies and Sequential Point Trees.

3.1 3D Gaussian Splatting

3D Gaussian Splatting [Kerbl et al. 2023] models a radiance field using a set of spatially distributed Gaussians, each with mean $\mu_i \in \mathbb{R}^3$, RGB base colors $b_i \in \mathbb{R}^3$ and covariance matrices $\Sigma_i \in \mathbb{R}^{3 \times 3}$. The covariance is parameterized via a diagonal scaling matrix $S_i = \text{diag}(s_i^1, s_i^2, s_i^3)$ and an orthonormal rotation matrix R_i :

$$\Sigma_i = R_i S_i S_i^\top R_i^\top.$$

Each Gaussian also stores an opacity σ_i and view-dependent color, modeled using spherical harmonics (SH) coefficients f_i^d . The SH degree d controls expressiveness, with each Gaussian requiring $\sum_{j=1}^d 3 \cdot (2j + 1)$ parameters. For rendering, all N Gaussians are sorted by distance to the camera and a discrete approximation of the volume rendering equation is evaluated for every pixel x with

corresponding view direction v :

$$C(x) = \sum_{i=1}^N c_i(v) \alpha_i(x) \prod_{j=1}^{i-1} (1 - \alpha_j(x)),$$

where α_j is the opacity of the j -th Gaussian along the view ray:

$$\alpha_j(x) = \sigma_j e^{-\frac{1}{2}(x - \mu'_j) \Sigma' (x - \mu'_j)^T}.$$

Here μ' and Σ' denote the projected 2D mean and covariance on the image plane, obtained by applying an affine approximation of the projective transform [Zwicker et al. 2001]. The rendering pipeline is fully differentiable, enabling end-to-end optimization with ADAM using a combination of \mathcal{L}_1 and SSIM losses.

3.2 Memory in 3DGS

Standard 3DGS pipelines store the full set of per-Gaussian attributes, training images, and optimizer state in GPU memory (VRAM). Figure 15 summarises the amount of memory that the various components of a single Gaussian require. Additional temporary allocations occur during forward and backward passes (e.g., for sorting and gradient accumulation). This overhead varies with the scale of the Gaussians and effectiveness of culling strategies, but can be roughly upper-bounded by around 800 bytes per Gaussian in practice. This limits training to roughly 500K Gaussians per GB of VRAM, imposing strict constraints on the detail and extent of reconstructions.

3.3 Gaussian Hierarchies and Sequential Point Trees

Gaussian hierarchies, introduced in [Kerbl et al. 2024], recursively merge nearby Gaussians into a tree, where each non-leaf node approximates its children, and leaves correspond to the original Gaussians. A cut is defined by a condition $c_{\text{hier}}(i, \text{cam})$ evaluated in a breadth-first search (BFS). If a node satisfies the cut condition, it is added to the cut set and its children are skipped; otherwise, the BFS continues. A *proper cut set* includes no parents or children of any included node and thus provides a view-adaptive LoD representation.

The cut condition used in [Kerbl et al. 2024] is:

$$c_{\text{hier}}(i, \text{cam}) = \|\mu_i - \mathbf{p}_{\text{cam}}\|_2 \geq m_d(i), \quad m_d(i) = \frac{T}{\max_j s_i^j},$$

where \mathbf{p}_{cam} is the camera position, T is a global LoD threshold, and $m_d(i)$ is the minimum acceptable distance for viewing Gaussian i . This ensures that if i is in the cut set, its parent failed the condition:

$$m_d(\text{parent}(i)) > \|\mu_i - \mathbf{p}_{\text{cam}}\|_2 \geq m_d(i).$$

Sequential Point Trees (SPTs) [Dachsbacher et al. 2003], originally developed for point cloud LoD rendering, can be adapted for Gaussians. They enforce a more constrained cut condition:

$$c_{\text{SPT}}(i, \text{cam}) = m_d(\text{parent}(i)) > \|\mu_{\text{root}} - \mathbf{p}_{\text{cam}}\|_2 \geq m_d(i).$$

This condition is evaluated for all Gaussians in parallel, using the shared root-camera distance $\|\mu_{\text{root}} - \mathbf{p}_{\text{cam}}\|_2$. It requires storing only sorted pairs $(m_d(i), m_d(\text{parent}(i)))$, significantly reducing memory compared to full Gaussian hierarchies. Note that cuts are guaranteed to be proper, with nodes where $m_d(i) < m_d(\text{parent}(i))$ never being selected for the cut. To optimize cuts, Gaussians are sorted by $m_d(\text{parent}(i))$ in descending order. A binary search determines

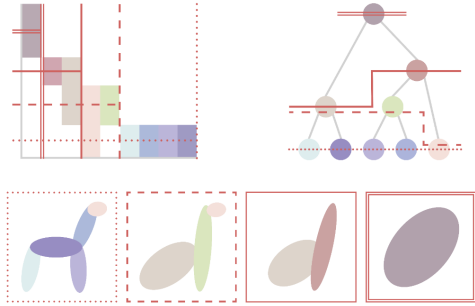


Fig. 2. A Sequential Point Tree and Gaussian hierarchy represent the same 5 Gaussians at varying levels of detail shown with four possible hierarchy cuts in red. Horizontal lines in the SPT show the binary search result and horizontal lines the distance cut.

the cutoff index N , above which Gaussians are too fine to be rendered. The downside of the approach is that all Gaussians in the same SPT share the same level of detail dictated by the distance from the camera to the root node. This can lead to Gaussians with $m_d(i) > \|\mu_i - \mathbf{p}_{\text{cam}}\|_2$ being rendered, even though they would be too coarse for the current view. To counteract this issue, we define:

$$M_d(i) = m_d(i) + \|\mu_i - \mathbf{p}_{\text{cam}}\|_2,$$

as a conservative minimum distance function. By the triangle inequality, selecting Gaussians satisfying $M_d(i) \leq \|\mu_{\text{root}} - \mathbf{p}_{\text{cam}}\|_2$ guarantees $m_d(i) \leq \|\mu_i - \mathbf{p}_{\text{cam}}\|_2$. In turn, this means that Gaussians that are further away from the camera than the root node will be selected at a higher level of detail. SPTs are best suited for tightly grouped Gaussians observed from distances greater than their mutual spacing. Their compact memory footprint and parallel evaluation make them well-suited for large-scale scenes. Figure 2 visualizes both hierarchy types and their LoD cuts for a toy example.

4 Method

An overview of the training and densification process can be found in Figure 7, where we enumerate the individual steps of our training and densification process: To train models exceeding GPU memory limits, all Gaussian attributes are stored in CPU RAM and streamed to the GPU on demand for each training view. To accelerate the hierarchy cut, we store a copy of only the tree structure in VRAM, where larger subtrees have been replaced by SPTs, forming a *hierarchical SPT (HSPT)*. To minimize costly transfers between RAM and VRAM, we keep track of which SPTs are currently loaded and at which detail, and cache them in GPU memory. Only if an SPT is not present in this GPU cache at a similar level of detail, will it be loaded from RAM. Densification occurs on the CPU by adding new leaf nodes to the hierarchy and respawning low-opacity leaf nodes. The densified hierarchy is then converted back to an HSPT and transferred to the GPU for a new round of training iterations.

4.1 Initialization

Following Kerbl et al. [2024], we initialize the Gaussian model from a sparse point cloud, augmented with skybox points. This initial representation is small enough to fully reside in GPU memory and

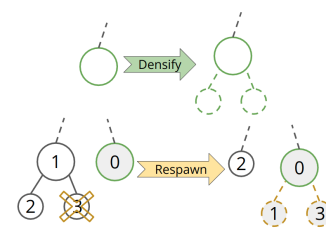


Fig. 3. Example of densifying and respawning leaf nodes.

is trained for 100 000 iterations with densification disabled. The goal of this phase is to establish a stable global scene structure before hierarchy construction. After this initial optimization, we build a binary Gaussian hierarchy, with the trained Gaussians as leaf nodes and parent nodes representing merged approximations of their children.

4.2 Gradient Propagation

To update the properties of Gaussians, including base color, SH coefficients, position, and covariance, we follow the standard 3DGS error propagation [Kerbl et al. 2023]. However, we operate only on the cut set chosen for each training view. Thus, gradients may, in general, be propagated to Gaussians in the middle of the hierarchy.

4.3 Densification

Densifying a Level-of-Detail representation presents a unique challenge: the underlying hierarchical structure must evolve continuously during training. Prior works circumvent this issue by constructing LoD hierarchies only after chunk-level training and densification are complete.

We take inspiration from 3DGS-MCMC [Kheradmand et al. 2024], which selects Gaussians probabilistically (weighted by opacity) to be ‘split’, replacing it by two new Gaussians which together should appear similarly to the original split Gaussian. Noteably, this resembles the way a parent node in a Gaussian hierarchy approximates its children. Therefore, we adopt this approach and ‘spawn’ two new child nodes for a leaf instead of splitting a Gaussian, increasing the size of the hierarchy with minimal artifacts.

Instead of pruning, Kheradmand et al. [2024] declares Gaussians below a certain opacity threshold as ‘dead’, and respawns them at the position of a high-opacity Gaussian. We propose a similar strategy: when a leaf node dies, its parent is replaced by its sibling node; the dead leaf node and its parent are then respawned as children to another node, which is selected to be densified. See Figure 3 for an overview of the two hierarchy densification operations. Together, they ensure that the hierarchy can be expanded during training in a stable manner and rebalanced as required. Avoiding destructive resets, as advocated by Kerbl et al. [2023], is particularly important in our setting, as many Gaussians will no longer conform to the hierarchical structure after opacity is restored to normal.

4.4 The hierarchical SPT datastructure

BFS. Computing the cut set of a large Gaussian hierarchy is a costly operation that must be performed for every frame. A straightforward solution is to run a breadth-first search (BFS) from the root. This guarantees a proper cut and enables early pruning of large subtrees, e.g., via frustum culling. However, graph traversal is not well suited to parallel execution on the GPU.

Parallel Cut. To enable GPU-accelerated cuts, Kerbl et al. [2024] evaluate the cut condition in parallel for each Gaussian:

$$(m_d(i) < \|\mu_i - \mathbf{p}_{cam}\|_2) \wedge (m_d(\text{parent}(i)) \geq \|\mu_{\text{parent}(i)} - \mathbf{p}_{cam}\|_2),$$

where any Gaussian that is sufficiently small at its current camera distance and whose parent is too large to be rendered, should be part of the cut set. This produces a proper cut under the assumption that child Gaussians always have a smaller minimal distance than their parents:

$$\forall i : m_d(i) < m_d(\text{parent}(i)).$$

This is generally valid when hierarchies are constructed after training, since parent Gaussians represent coarser approximations of their children. However, when the hierarchy is modified during training and densification, optimization can cause this assumption to break—leading to invalid cut sets and degenerate hierarchies that worsen over time.

Hierarchical SPT (HSPT). We present the hierarchical SPT data structure, which combines the benefits of both approaches. To construct it, we cut it using a BFS on the condition

$$c_{HSPT}(i) = s_i^1 \cdot s_i^2 \cdot s_i^3 < \text{size}$$

with volume threshold *size*. The resulting cut set \mathbb{C}_{HSPT} partitions the hierarchy into the *upper hierarchy*, which includes all Gaussians with volume greater than *size*, and the *lower hierarchy*, consisting of the subtrees rooted at the nodes in the cut set.

The volume of each root node in the lower hierarchy is now bounded by *size*, which also roughly bounds the extent of all Gaussians in the subtree. This provides an upper bound on the error introduced if the subtree is converted into an SPT. Consequently, each subtree of sufficient size in \mathbb{C}_{HSPT} can be transformed into a Sequential Point Tree to accelerate cut computation. The HSPT-based cutting process then proceeds in two steps: first, a BFS on the upper hierarchy selects the required nodes and leaf/SPT subtrees for the current view. Second, each selected SPT is cut according to the camera’s distance to its root node. Together, these yield the full set of Gaussians needed for rendering the current frame.

The construction and cutting process of an HSPT is illustrated in Figure 4. The SPTs used to render a MatrixCity-Scale frame are shown in Figure 11, and Figure 10 demonstrates the smooth LoD transitions enabled by the hierarchical structure.

Rebuilding the hierarchical SPT for every training iteration would eliminate any performance benefit. Instead, we exploit the fact that the minimum distance m_d evolves slowly during optimization and thus only needs to be updated infrequently. In practice, we rebuild the HSPT only after each densification step.

This infrequent recomputation allows us to use a more accurate—albeit more expensive—minimum distance metric than the inverse

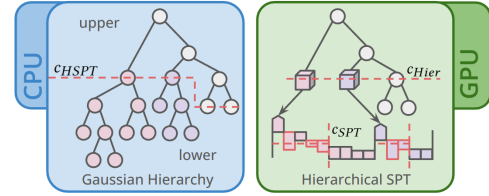


Fig. 4. A Gaussian hierarchy is converted to an HSPT by cutting according to Gaussian volume and converting sufficiently large subtrees to SPTs. The HSPT can then be cut in a 2-step process.

of maximal scale. Specifically, we define:

$$m'_d(i) = \frac{T}{\sqrt{s_i^1 \cdot s_i^2 + s_i^1 \cdot s_i^3 + s_i^2 \cdot s_i^3}},$$

which corresponds to the inverse square root of the surface area of the Gaussian ellipsoid (up to a constant factor). This better captures the perceived size of anisotropic Gaussians, especially those that are significantly elongated in one or more directions.

Frustum Culling. The major benefits of using BFS to cut the upper hierarchy are the guarantee of a proper cut and early culling of subtrees. To this end, we frustum cull every node considered in the BFS by checking if a sphere around the Gaussians with radius equal to $(3 \cdot \max_j s_i^j)$ intersects with the view frustum. Using the Gaussian scale as a proxy for the extent of its entire subtree is not perfectly accurate, but comparisons to using a full bounding sphere hierarchy showed no discernable difference in practice. It should be noted that Gaussians are implicitly frustum culled during rasterization, but this early culling accelerates the cutting procedure and significantly decreases the number of Gaussians that need to be loaded from RAM, as can be seen in Figure 9.

4.5 Caching on the GPU

Loading Gaussian data from RAM is a costly operation that can become a significant bottleneck during large-scale training. To mitigate this, we maintain a GPU-resident cache of Gaussians that are likely to be reused across consecutive training views. However, checking the cache for every individual Gaussian would introduce nontrivial overhead. Once again, SPTs offer an efficient alternative.

Rather than caching individual Gaussians, we store the Gaussians from SPT cuts along with the cached distance from the camera to the root of each SPT, denoted \bar{d}^j for the j th SPT. During rendering, when the upper hierarchy is cut and the required SPTs identified, we compute $d^j = \|\mu_{\text{root}(j)} - \mathbf{p}_{cam}\|_2$ and check whether a matching cut is already cached. This check is performed using a simple distance ratio tolerance:

$$D_{\min} \leq \frac{d^j}{\bar{d}^j} \leq D_{\max}.$$

Here, D_{\max} defines the allowable range for using coarser-than-optimal detail, while D_{\min} limits how much finer detail can be tolerated. If this condition is met, the cached SPT cut is reused, avoiding a costly RAM-to-GPU transfer. While this heuristic introduces slight variability in rendered detail—since the LoD may depend on the cache state—we find that this stochasticity actually

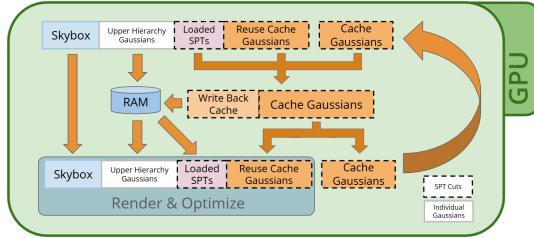


Fig. 5. Caching strategy overview. Gaussians required for the current training view are assembled from three sources: the upper tree, newly loaded SPT cuts from RAM, and cache hits. After optimization, newly accessed SPTs are added to the GPU cache.

improves training robustness. In particular, the subtle variation in detail across views discourages overfitting to fixed camera distances and promotes better generalization across scales.

For each training view, visible Gaussians are assembled from the upper hierarchy, the cached SPTs, and the skybox Gaussians (which remains in VRAM). Uncached SPTs are streamed from RAM. After each training iteration, newly loaded SPTs are added to the cache.

To bound VRAM usage, we use a least-recently-used (LRU) write-back policy. When a memory threshold is exceeded, entries are written back to RAM. Additionally, to prevent overfitting to persistent cache entries, the entire cache is flushed every 1 000 iterations. Figure 5 illustrates the caching process across two frames.

View Selection. In large-scale scenes, the GPU cache typically covers only a small fraction of the overall geometry, leading to sparse cache hits. To improve cache utilization, we prioritize spatial locality by selecting successive training views that are geographically close to the current one, thereby maximizing Gaussian reuse.

To this end, we precompute a k -nearest-neighbor graph over all training view positions, where edge weights w_{ij} correspond to the Euclidean distance between views i and j . The next training view j is then sampled from the k -nearest neighbors of the current view i according to the distribution:

$$\mathbb{P}(j | i) \propto \frac{1}{w_{ij} + W},$$

where W is a constant, controlling the degree of exploration.

However, care must be taken when modifying the order of training views, as deviating from uniform random sampling may introduce bias. Thus, we inject a random view every 12 iterations, which we find sufficient to preserve generalization performance.

4.6 Memory Layout

Figure 6 illustrates the peak memory usage for a single training iteration of a 60-million-Gaussian hierarchy on the MatrixCity-Scale dataset. The output frame from this iteration is shown in Figure 12. The majority of RAM usage is consumed by per-Gaussian properties and their corresponding ADAM optimizer states. In contrast, the hierarchy structure itself accounts for less than 10% of the total RAM footprint. On the GPU, the SPT metadata for all 60 million Gaussians occupies just 680 MB of VRAM and the upper hierarchy negligible 24 MB.

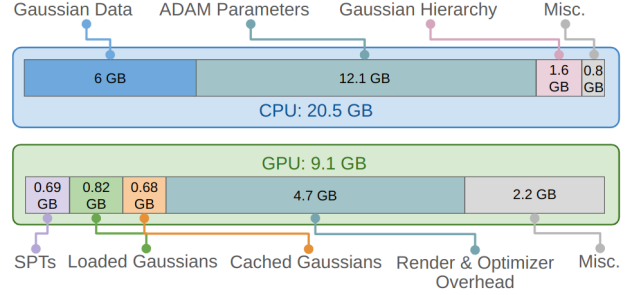


Fig. 6. Peak memory consumption of CPU and GPU for a training iteration on BigCity-Scale with 60 million Gaussians.

Even in wide-angle aerial views, only a subset of the scene is actively loaded into GPU memory. In the example shown, 2.2 million Gaussians are rendered directly, while an additional 2.4 million are retained in the cache for future use. The bulk of GPU memory is instead consumed by temporary allocations for rasterization and optimization, which scale with the number of Gaussians rendered. Therefore, minimizing the number of active Gaussians is critical for staying within the VRAM budget.

The remaining GPU memory usage consists of auxiliary data, including cache management, hierarchy cut tracking, training and ground-truth images, as well as PyTorch overhead. Figure 15 provides a breakdown of memory usage for Gaussian properties and hierarchy data, and how these are distributed across CPU and GPU.

5 Evaluation

Choice of dataset. Our method is designed to enable seamless training and rendering on large-scale scenes comprising thousands of views captured at vastly different scales. Unfortunately, most existing datasets of sufficient size contain either street-level or aerial views—but not both. Additionally, at this scale and density, current Structure-from-Motion (SfM) pipelines often fail to reliably recover camera poses and sparse point clouds.

To overcome these challenges, we use the synthetic *MatrixCity* dataset [Li et al. 2023], which provides dense multi-scale views along with ground-truth camera poses and sparse geometry. For our main benchmark, *MatrixCity-Scale* (MC-Scale), we aggregate 11 466 street-view images, 3 208 aerial views, and 533 additional high-altitude views we generate manually. We evaluate reconstruction quality on a separate set of 1 694 test images. The diversity in image scale is visualized in Figure 8. To validate our method on real-world data, we also include results on the largest public dataset from Kerbl et al. [2024], the *Campus* scene.

Choice of Comparison. Selecting appropriate baselines is challenging. Standard 3DGS variants perform poorly at large scales, while most divide-and-conquer approaches—such as Hierarchical 3DGS, CityGS, and HorizonGS—assume access to 80 GB GPUs. Despite access to multiple clusters, we were limited to 40 GB A100s, highlighting the hardware demands of these methods.

To our knowledge, only Hierarchical 3DGS has trained successfully on the Campus dataset, and no prior work has demonstrated

large-scale training on MatrixCity with combined aerial and street views. Due to resource constraints, we were unable to train CityGS on either dataset and adopt Hierarchical 3DGS as our main baseline.

For additional reference, we evaluate 3DGS-MCMC, modified to support large-scale training by limiting densification, streaming images from disk, and reducing the SH degree. Most chunk-based methods, including Kerbl et al. [2024], require feature correspondences, which are not provided in MatrixCity. To enable comparison, we reconstructed a sparse point cloud using COLMAP and the provided camera poses. This less stable point cloud (visualized in Figure 8) was used for initialization.

On the Campus scene, we report results for the official test split (Hierarchical single) and the full pretrained model. Consequently, we evaluate reconstruction quality on every 100th training view. We train a smaller model (38M) and a larger (80M) model. Rendering Hierarchical 3DGS required reducing SH degree to 1—even on 40 GB VRAM; ours also uses SH degree 1. Given the limitations of numerical metrics in these settings, we strongly encourage visual comparison via the supplementary videos, which in our opinion favour Hierarchical 3DGS. Except for the results of Hierarchical 3DGS, all training and rendering was done using an RTX 3090 GPU.

5.1 Results

Quantitative comparisons are shown in Table 1. *A LoD of Gaussians* successfully reconstructs the full MC-Scale scene, where other methods struggle due to the scene’s size and diverse camera viewpoints. Notably, Kerbl et al. [2024] reconstructs individual chunks accurately, but the merging process introduces “floaters”—isolated Gaussians not associated with meaningful geometry—which obscure most test views (see Figure 13 and 14). Similarly, 3DGS-MCMC suffers from aggressive opacity and scale-based pruning, causing a large fraction of Gaussians to vanish entirely.

On the *Campus* dataset, Hierarchical 3DGS performs well, as its chunk-based approach aligns with the dataset’s single, street-level trajectory. Their single-chunk evaluation shows strong metrics. However, when evaluating their full model with reduced SH degree (to fit within 40 GB VRAM), we observe a clear drop in numerical quality. That said, the visual results remain competitive—see the supplemental video. In our case, both low- and high-resolution variants achieve similar quantitative scores despite visible differences, due to Hierarchical 3DGS evaluating on training views.

For context, Hierarchical 3DGS splits the MC-Scale scene into 94 chunks, each trained for 45 000 iterations, totaling over 4.23 million steps and nearly four full days of compute time on our machine. By contrast, our approach trains the full scene end-to-end in just 250 000 iterations, completing in approximately 15 hours.

Memory. A major limitation of chunk-based methods is the memory overhead during rendering. Although it also implements a form of GPU streaming, we were unable to run the viewer provided by Kerbl et al. [2024] on either dataset using the 40 GB VRAM A100, which is consistent with the limitations they report. In contrast, our method renders interactive flythroughs of MatrixCityScale and Campus (38M), see supplemental, while only requiring 8 GB of GPU memory (and 16 GB for Campus (80M)).

Table 1. **Full Novel View Synthesis results.** * use of the suboptimal COLMAP version for MC-Scale; \ddagger adjusted SH degree to match ours and reduce memory to enable rendering, \dagger use of higher SH degree and only single chunk, reproduced from [Kerbl et al. 2024].

Method	MC-Scale (15k images)				Campus (22k images)			
	PSNR \uparrow	SSIM \uparrow	LPIPS \downarrow	Size	PSNR \uparrow	SSIM \uparrow	LPIPS \downarrow	Size
Ours*	20.63	0.668	0.282	40M	22.83	0.713	0.248	38M
Hierarchical* \ddagger	13.77	0.519	0.559	82M	17.76	0.601	0.424	80M
Ours	21.73	0.712	0.213	60M	22.86	0.725	0.237	80M
Hierarchical single \dagger					24.61	0.807	0.331	-
3DGS-MCMC	13.16	0.4481	0.586	6M	15.11	0.600	0.580	6M

Table 2. **Ablations.** Average frame times for rendering camera paths and average iteration times during training with and without caching Gaussians. Then, average times to cut the hierarchy during rendering with the normal BFS approach and HSPT. 80M Campus was trained longer than 38M.

	MC-Scale	Campus	
		38M	80M
Render Full	48.1 ms	47.1 ms	83.2 ms
Render w/o Cache	119.4 ms	92.6 ms	222.3ms
Render w/o Frustum Culling	52.3 ms	38.3 ms	110.2 ms
Train Full	156 ms	205 ms	
Train w/o Cache	471 ms	244 ms	
Train w/o Frustum Culling	685 ms	312 ms	
HSPT Cut (Render)	31.9 ms	31.3 ms	36.5 ms
BFS Cut (Render)	47.8 ms	40.0 ms	53.7 ms

5.2 Ablations

We assess the contribution of key components through an ablation study, using recorded camera paths across all scenes (see supplemental video). Table 2 reports average frame times over these paths. Caching significantly improves performance, roughly doubling the framerate across scenes. Frustum culling is particularly beneficial for large-scale models but may incur overhead in smaller scenes. To evaluate cut efficiency, we compare the time required to compute the visible set using either full hierarchy BFS or our HSPT-based approach. HSPT consistently yields faster cut times. For training, we measure average iteration durations over 1 000 steps. Here, frustum culling again proves essential, substantially reducing the number of Gaussians loaded and processed per view.

View Selection. On the MatrixCity-Scale dataset (250K iterations, up to 60M Gaussians), enabling view selection reduces the number of Gaussians loaded from RAM per frame from 355K to 219K—a 35% reduction in memory load. Reconstruction quality is unaffected, with PSNR and SSIM improving slightly by 0.04 and 0.05, respectively.

6 Discussion and Outlook

A LoD of Gaussians enables seamless training and rendering of ultra-large 3DGS models on consumer hardware. By storing Gaussian data in external memory and streaming it on demand, our method avoids the pitfalls of chunk-based pipelines. The hierarchical SPT structure accelerates LoD selection and remains robust to ongoing training changes. Combined with caching and view selection, our system significantly reduces out-of-core overhead. Together, these components enable efficient reconstruction and rendering at scale, demonstrated on the MatrixCity-Scale dataset.

Limitations and Future Work. A primary limitation of our method lies in initialization. Accurate estimation of camera poses and sparse point clouds remains challenging at large scale, particularly for real-world datasets with sparse or inconsistent coverage. Future work could explore improved initialization strategies or joint optimization of poses and Gaussians during early training.

Our system also requires roughly 1 GB of RAM per million Gaussians, which—while more efficient than prior methods—still constrains scalability. Loading from disk is feasible in our experiments, though at the cost of a 10× slowdown. Preliminary exploration has also shown that given access to sufficient RAM and training time, our method could scale far beyond what is presented here. A 150 million Gaussian model has been trained successfully for MatrixCity-Scale on 24 GB of VRAM, though the improvement to image quality was minor. We suspect that even more training views are required to properly leverage such a vast number of Gaussians.

Rendering could be further optimized by avoiding per-frame hierarchy cut recomputation and enabling asynchronous streaming. While frustum culling reduces memory load in most views, it is ineffective when the entire scene falls inside the frustum. Occlusion culling could address this by skipping entire SPTs before loading.

Overall, we believe that out-of-core 3D Gaussian Splatting is a promising direction for scaling radiance field methods to city-scale and beyond, without the need for specialized hardware.

References

Sameer Agarwal, Noah Snavely, Ian Simon, Steven M. Seitz, and Richard Szeliski. 2009. Building Rome in a day. In *2009 IEEE 12th International Conference on Computer Vision*. 72–79. doi:10.1109/ICCV.2009.5459148

Junyi Chen, Weicai Ye, Yifan Wang, Danpeng Chen, Di Huang, Wanli Ouyang, Guofeng Zhang, Yu Qiao, and Tong He. 2024b. GigaGS: Scaling up Planar-Based 3D Gaussians for Large Scene Surface Reconstruction. arXiv:2409.06685 [cs.CV] <https://arxiv.org/abs/2409.06685>

Yihang Chen, Qianyi Wu, Weiyao Lin, Mehrtash Harandi, and Jianfei Cai. 2024a. Hac: Hash-grid assisted context for 3d gaussian splatting compression. In *European Conference on Computer Vision*. Springer, 422–438.

Kai Cheng, Xiaoxiao Long, Kaizhi Yang, Yao Yao, Wei Yin, Yuxin Ma, Wenping Wang, and Xuejin Chen. 2024. Gaussianpro: 3d gaussian splatting with progressive propagation. In *Forty-first International Conference on Machine Learning*.

Carsten Dachsibacher, Christian Vogelsang, and Marc Stamminger. 2003. Sequential point trees. *ACM Trans. Graph.* 22, 3 (July 2003), 657–662. doi:10.1145/882262.882321

Zhiwen Fan, Kevin Wang, Kairun Wen, Zehao Zhu, Dejia Xu, and Zhangyang Wang. 2024. LightGaussian: Unbounded 3D Gaussian Compression with 15x Reduction and 200+ FPS. arXiv:2311.17245 [cs.CV] <https://arxiv.org/abs/2311.17245>

Guangchi Fang and Bing Wang. 2024. Mini-Splatting: Representing Scenes with a Constrained Number of Gaussians. arXiv:2403.14166 [cs.CV] <https://arxiv.org/abs/2403.14166>

Sharath Girish, Kamal Gupta, and Abhinav Shrivastava. 2024. Eagles: Efficient accelerated 3d gaussians with lightweight encodings. In *European Conference on Computer Vision*. Springer, 54–71.

He Huang, Wenjie Huang, Qi Yang, Yiling Xu, and Zhu li. 2025. A Hierarchical Compression Technique for 3D Gaussian Splatting Compression. arXiv:2411.06976 [cs.CV] <https://arxiv.org/abs/2411.06976>

Lihan Jiang, Kerui Ren, Mulin Yu, Linning Xu, Junting Dong, Tao Lu, Feng Zhao, Dahua Lin, and Bo Dai. 2024. Horizon-GS: Unified 3D Gaussian Splatting for Large-Scale Aerial-to-Ground Scenes. arXiv:2412.01745 [cs.CV] <https://arxiv.org/abs/2412.01745>

Bernhard Kerbl, Georgios Kopanas, Thomas Leimkühler, and George Drettakis. 2023. 3D Gaussian Splatting for Real-Time Radiance Field Rendering. *ACM Transactions on Graphics (SIGGRAPH Conference Proceedings)* 42, 4 (July 2023). <http://www-sop.inria.fr/reves/Basilic/2023/KKLD23>

Bernhard Kerbl, Andreas Meuleman, Georgios Kopanas, Michael Wimmer, Alexandre Lanvin, and George Drettakis. 2024. A Hierarchical 3D Gaussian Representation for Real-Time Rendering of Very Large Datasets. *ACM Trans. Graph.* 43, 4, Article 62 (July 2024), 15 pages. doi:10.1145/3658160

Shakiba Kheradmand, Daniel Rebain, Gopal Sharma, Weiwei Sun, Yang-Che Tseng, Hossam Isack, Abhishek Kar, Andrea Tagliasacchi, and Kwang Moo Yi. 2024. 3D Gaussian Splatting as Markov Chain Monte Carlo. In *Advances in Neural Information Processing Systems*, A. Globerson, L. Mackey, D. Belgrave, A. Fan, U. Paquet, J. Tomczak, and C. Zhang (Eds.), Vol. 37. Curran Associates, Inc., 80965–80986. https://proceedings.neurips.cc/paper_files/paper/2024/file/93be245fce00a9bb2333c17ceae4b732-Paper-Conference.pdf

Sieun Kim, Kyungjin Lee, and Youngki Lee. 2024. Color-cued Efficient Densification Method for 3D Gaussian Splatting. In *Proceedings of the IEEE/CVF Conference on Computer Vision and Pattern Recognition*. 775–783.

Joo Chan Lee, Daniel Rho, Xiangyu Sun, Jong Hwan Ko, and Eunbyung Park. 2024. Compact 3d gaussian representation for radiance field. In *Proceedings of the IEEE/CVF Conference on Computer Vision and Pattern Recognition*. 21719–21728.

Ruiling Li, Sanja Fidler, Angjoo Kanazawa, and Francis Williams. 2024. NeRF-XL: Scaling NeRFs with Multiple GPUs. arXiv:2404.16221 [cs.CV] <https://arxiv.org/abs/2404.16221>

Yixuan Li, Lihan Jiang, Linning Xu, Yuanbo Xiangli, Zhenzhi Wang, Dahua Lin, and Bo Dai. 2023. MatrixCity: A Large-scale City Dataset for City-scale Neural Rendering and Beyond. arXiv:2309.16553 [cs.CV] <https://arxiv.org/abs/2309.16553>

Zhuoxiao Li, Shanliang Yao, Yong Yue, Wufan Zhao, Rongjun Qin, Angel F. Garcia-Fernandez, Andrew Levers, and Xiaohui Zhu. 2025. ULSR-GS: Ultra Large-scale Surface Reconstruction Gaussian Splatting with Multi-View Geometric Consistency. arXiv:2412.01402 [cs.CV] <https://arxiv.org/abs/2412.01402>

Jiaqi Li, Zhihao Li, Xiao Tang, Jianzhuang Liu, Shiyong Liu, Jiayue Liu, Yangdi Lu, Xiaofei Wu, Songcen Xu, Youliang Yan, and Wenming Yang. 2024. VastGaussian: Vast 3D Gaussians for Large Scene Reconstruction. arXiv:2402.17427 [cs.CV] <https://arxiv.org/abs/2402.17427>

Rong Liu, Rui Xu, Yue Hu, Meida Chen, and Andrew Feng. 2024c. Atomgs: Atomizing gaussian splatting for high-fidelity radiance field. *arXiv preprint arXiv:2405.12369* (2024).

Xiangrui Liu, Xinju Wu, Pingping Zhang, Shiqi Wang, Zhu Li, and Sam Kwong. 2024b. Compgs: Efficient 3d scene representation via compressed gaussian splatting. In *Proceedings of the 32nd ACM International Conference on Multimedia*. 2936–2944.

Yang Liu, He Guan, Chuanchen Luo, Lue Fan, Naiyan Wang, Junran Peng, and Zhaoxiang Zhang. 2024a. CityGaussian: Real-time High-quality Large-Scale Scene Rendering with Gaussians. arXiv:2404.01133 [cs.CV] <https://arxiv.org/abs/2404.01133>

Yang Liu, Chuanchen Luo, Zhongkai Mao, Junran Peng, and Zhaoxiang Zhang. 2025. CityGaussianV2: Efficient and Geometrically Accurate Reconstruction for Large-Scale Scenes. arXiv:2411.00771 [cs.CV] <https://arxiv.org/abs/2411.00771>

Tao Lu, Mulin Yu, Linning Xu, Yuanbo Xiangli, Limin Wang, Dahua Lin, and Bo Dai. 2023. Scaffold-GS: Structured 3D Gaussians for View-Adaptive Rendering. arXiv:2312.00109 [cs.CV] <https://arxiv.org/abs/2312.00109>

Saswat Subhajyoti Mallick, Rahul Goel, Bernhard Kerbl, Markus Steinberger, Francisco Vicente Carrasco, and Fernando De La Torre. 2024. Taming 3dgs: High-quality radiance fields with limited resources. In *SIGGRAPH Asia 2024 Conference Papers*. 1–11.

Ben Mildenhall, Pratul P. Srinivasan, Matthew Tancik, Jonathan T. Barron, Ravi Ramamoorthi, and Ren Ng. 2020. NeRF: Representing Scenes as Neural Radiance Fields for View Synthesis. arXiv:2003.08934 [cs.CV] <https://arxiv.org/abs/2003.08934>

K Navaneeth, Kossar Pourrahimi Meibodi, Soroush Abbasi Koohpayegani, and Hamed Pirsiavash. 2023. Compact3d: Compressing gaussian splat radiance field models with vector quantization. *arXiv preprint arXiv:2311.18159* 4 (2023).

Simon Niedermayr, Josef Stumpfegger, and Rüdiger Westermann. 2024. Compressed 3D Gaussian Splatting for Accelerated Novel View Synthesis. arXiv:2401.02436 [cs.CV] <https://arxiv.org/abs/2401.02436>

Michael Niemeyer, Fabian Manhardt, Marie-Julie Rakotosaona, Michael Oechslé, Daniel Duckworth, Rama Gosula, Keisuke Tateno, John Bates, Dominik Kaeser, and Federico Tombari. 2025. RadSplat: Radiance Field-Informed Gaussian Splatting for Robust Real-Time Rendering with 900+ FPS. arXiv:2403.13806 [cs.CV] <https://arxiv.org/abs/2403.13806>

Panagiotis Papantoniakis, Georgios Kopanas, Bernhard Kerbl, Alexandre Lanvin, and George Drettakis. 2024a. Reducing the memory footprint of 3d gaussian splatting. *Proceedings of the ACM on Computer Graphics and Interactive Techniques* 7, 1 (2024), 1–17.

Panagiotis Papantoniakis, Georgios Kopanas, Bernhard Kerbl, Alexandre Lanvin, and George Drettakis. 2024b. Reducing the Memory Footprint of 3D Gaussian Splatting. *Proceedings of the ACM on Computer Graphics and Interactive Techniques* 7, 1 (May 2024), 1–17. doi:10.1145/3651282

Kerui Ren, Lihan Jiang, Tao Lu, Mulin Yu, Linning Xu, Zhangkai Ni, and Bo Dai. 2024. Octree-GS: Towards Consistent Real-time Rendering with LOD-Structured 3D Gaussians. arXiv:2403.17898 [cs.CV] <https://arxiv.org/abs/2403.17898>

Johannes L. Schönberger and Jan-Michael Frahm. 2016. Structure-from-Motion Revisited. In *2016 IEEE Conference on Computer Vision and Pattern Recognition (CVPR)*. 4104–4113. doi:10.1109/CVPR.2016.445

Yunji Seo, Young Sun Choi, Hyun Seung Son, and Youngjung Uh. 2024. FLoD: Integrating Flexible Level of Detail into 3D Gaussian Splatting for Customizable Rendering. arXiv:2408.12894 [cs.CV] <https://arxiv.org/abs/2408.12894>

Matthew Tancik, Vincent Casser, Xinchen Yan, Sabeek Pradhan, Ben Mildenhall, Pratul P. Srinivasan, Jonathan T. Barron, and Henrik Kretzschmar. 2022. Block-NeRF: Scalable Large Scene Neural View Synthesis. arXiv:2202.05263 [cs.CV] <https://arxiv.org/abs/2202.05263>

Henan Wang, Hanxin Zhu, Tianyu He, Runsen Feng, Jiajun Deng, Jiang Bian, and Zhibo Chen. 2024b. End-to-end rate-distortion optimized 3d gaussian representation. In *European Conference on Computer Vision*. Springer, 76–92.

Yufei Wang, Zhihao Li, Lanqing Guo, Wenhan Yang, Alex Kot, and Bihan Wen. 2024a. Contextgss: Compact 3d gaussian splatting with anchor level context model. *Advances in neural information processing systems* 37 (2024), 51532–51551.

Linning Xu, Yuanbo Xiangli, Sida Peng, Xingang Pan, Nanxuan Zhao, Christian Theobalt, Bo Dai, and Dahua Lin. 2023. Grid-guided Neural Radiance Fields for Large Urban Scenes. arXiv:2303.14001 [cs.CV] <https://arxiv.org/abs/2303.14001>

Vickie Ye, Ruilong Li, Justin Kerr, Matias Turkulainen, Brent Yi, Zhuoyang Pan, Otto Seiskari, Jianbo Ye, Jeffrey Hu, Matthew Tancik, et al. 2025. gsplat: An open-source library for Gaussian splatting. *Journal of Machine Learning Research* 26, 34 (2025), 1–17.

Lingzhi Zhang, Tarmily Wen, and Jianbo Shi. 2019. Deep Image Blending. arXiv:1910.11495 [cs.CV] <https://arxiv.org/abs/1910.11495>

Hexu Zhao, Haoyang Weng, Daohan Lu, Ang Li, Jinyang Li, Aurojit Panda, and Saining Xie. 2024. On Scaling Up 3D Gaussian Splatting Training. arXiv:2406.18533 [cs.CV] <https://arxiv.org/abs/2406.18533>

Mathias Zwicker, Hanspeter Pfister, Jeroen van Baar, and Markus Gross. 2001. EWA Volume Splatting. In *IEEE Visualization*.

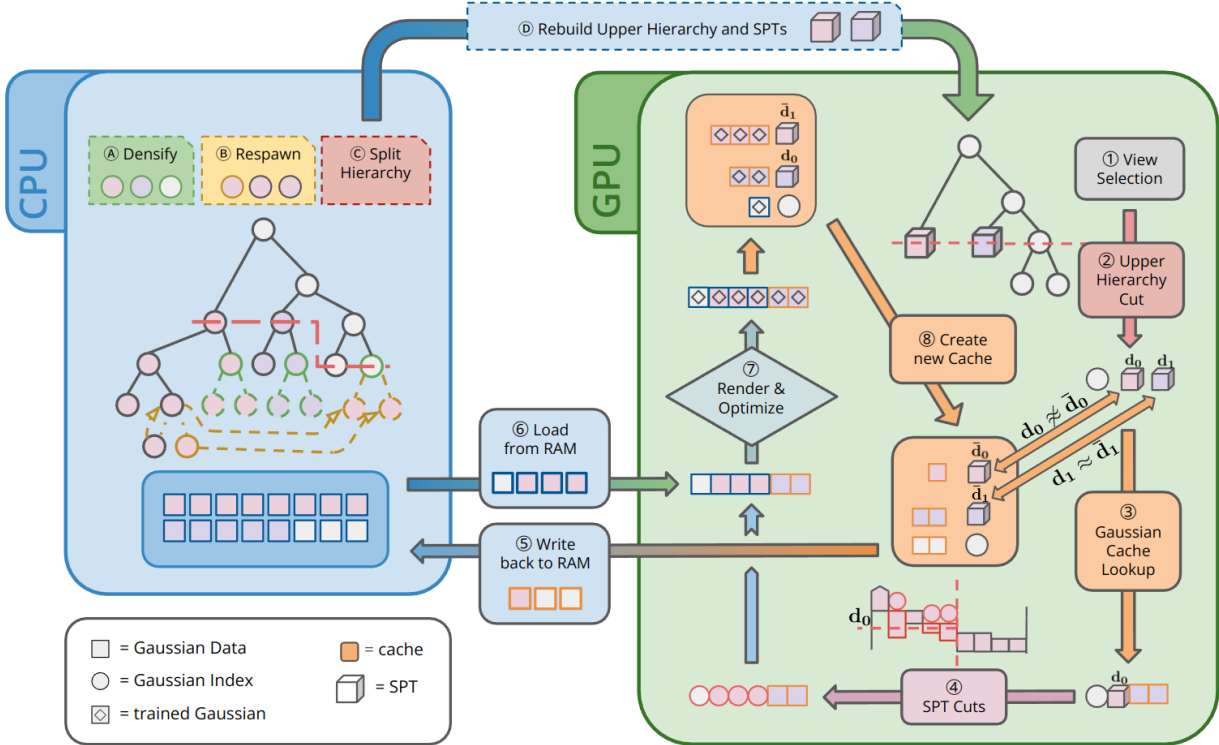


Fig. 7. Method Overview: Steps ① to ⑧ show the process of a single training iteration, while ⑨ through ⑪ show a densification step.

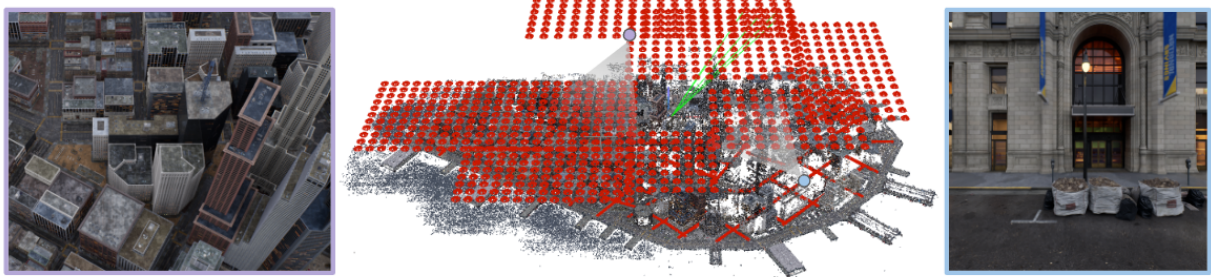


Fig. 8. Overview and examples of the street and aerial views (red) of the MatrixCity-Scale Dataset along with the COLMAP reconstruction (middle).



Fig. 9. Frustum Culling and LoD selection (left) greatly reduces the number of Gaussians required to render a view (right).

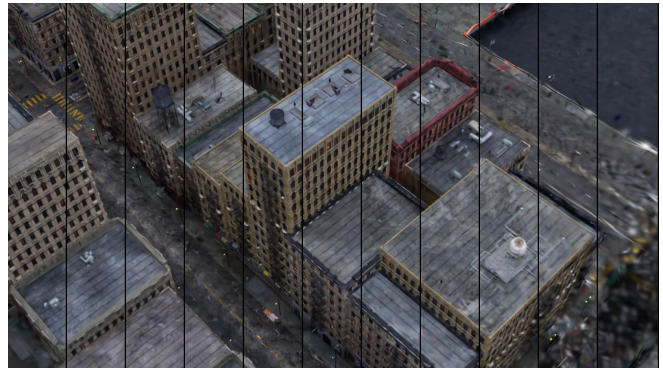


Fig. 10. Hierarchical SPTs enable smooth transitions between detailed (left) and coarse (right) representation.

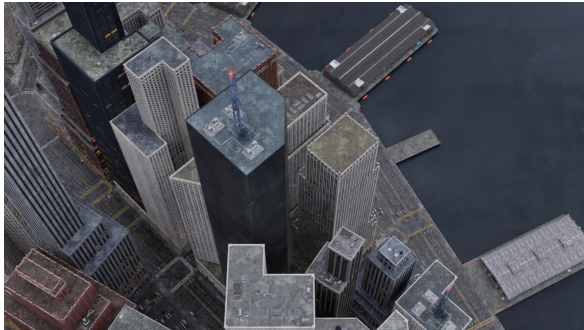
(a) Image generated during chunk training by *Hierarchical 3DGS*.(b) The same image generated during training by *A LoD of Gaussians*.

Fig. 14. Chunk-based optimizations causes floaters to expand outside of the chunk boundary.

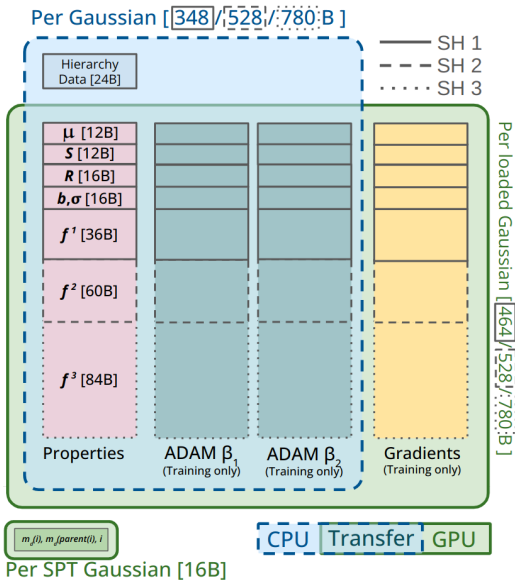


Fig. 15. All Gaussian properties except gradients are always present in CPU RAM, whereas only the currently loaded Gaussians and slim SPT information needs to be stored on GPU.

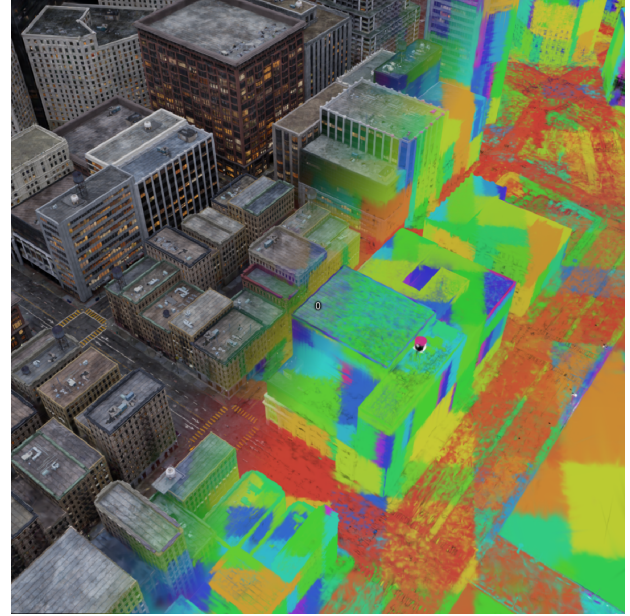


Fig. 11. SPTs for a frame of MatrixCity rendered in different colors.

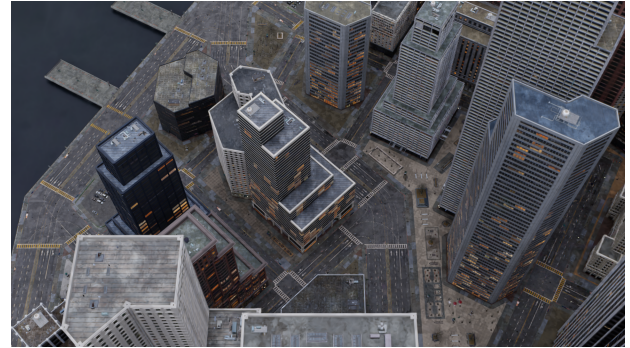


Fig. 12. Training image rendered during the iteration depicted in Figure 6.



Fig. 13. Images from Hierarchical 3DGS on the MatrixCity-Scale scene are obscured by large floaters.

Received 20 February 2007; revised 12 March 2009; accepted 5 June 2009